

# The Relationship between Anatomy and Photosynthetic Performance of Heterobaric Leaves<sup>1</sup>

Dimosthenis Nikolopoulos, Georgios Liakopoulos, Ioannis Drossopoulos, and George Karabourniotis\*

Laboratory of Plant Physiology, Department of Agricultural Biotechnology, Agricultural University of Athens, Iera Odos 75, 11855 Botanikos, Athens, Greece

Heterobaric leaves show heterogeneous pigmentation due to the occurrence of a network of transparent areas that are created from the bundle sheaths extensions (BSEs). Image analysis showed that the percentage of photosynthetically active leaf area ( $A_p$ ) of the heterobaric leaves of 31 plant species was species dependent, ranging from 91% in *Malva sylvestris* to only 48% in *Gynerium* sp. Although a significant portion of the leaf surface does not correspond to photosynthetic tissue, the photosynthetic capacity of these leaves, expressed per unit of projected area ( $P_{max}$ ), was not considerably affected by the size of their transparent leaf area ( $A_t$ ). This means that the photosynthetic capacity expressed per  $A_p$  ( $P_{max}^*$ ) should increase with  $A_t$ . Moreover, the expression of  $P_{max}^*$  could be allowing the interpretation of the photosynthetic performance in relation to some critical anatomical traits. The  $P_{max}^*$ , irrespective of plant species, correlated with the specific leaf transparent volume ( $\lambda_t$ ), as well as with the transparent leaf area complexity factor ( $^{CF}A_t$ ), parameters indicating the volume per unit leaf area and length/density of the transparent tissues, respectively. Moreover, both parameters increased exponentially with leaf thickness, suggesting an essential functional role of BSEs mainly in thick leaves. The results of the present study suggest that although the  $A_p$  of an heterobaric leaf is reduced, the photosynthetic performance of each areole is increased, possibly due to the light transferring capacity of BSEs. This mechanism may allow a significant increase in leaf thickness and a consequent increase of the photosynthetic capacity per unit (projected) area, offering adaptive advantages in xerothermic environments.

Plant tissues or single cells can behave as light guides or transparent windows, transferring light to the neighboring cells. Etiolated hypocotyls and coleoptiles as well as roots may guide light through the vacuoles and the cytoplasm of their cells, acting as bundles of optical fibers (Mandoli and Briggs, 1982, 1984a, 1984b). Sclereids, i.e. idioblastic cells within mesophyll of some sclerophylls, can also simulate single optical fibers, guiding light through the thick secondary wall to mesophyll areas with insufficient light supply (Karabourniotis et al., 1994; Karabourniotis, 1998). Thus, these fiber-like cells may contribute to the enhancement of the light microenvironment within internal mesophyll layers (Karabourniotis, 1998). Moreover, the leaves of some underground growing desert plants possess areas from which photosynthetic parenchyma layers are absent. The epidermis and the underlying water storage tissue in these window-leaved plants are transparent to allow light penetration to the internal chlorenchyma layers (Krulik, 1980). This anatomical adaptation presumably developed to allow photosynthesis underground so as to reduce water losses and heat load of the leaves.

Heterobaric leaves are characterized by the occurrence of transparent regions in the leaf blade that are easily seen as a network of bright lines on a dark green background under low magnification with transmitted light (McClendon, 1992). These transparent areas are created because the bundle sheaths of these leaves extend to the epidermis on both sides of the leaf, forming bundle sheath extensions (BSEs), which project as ribs on both surfaces of the lamina (Wylie, 1952; Esau, 1977; Fahn, 1990). As a consequence, the mesophyll of these plants is separated into many small compartments often termed "areoles" or "BSE compartments" (Terashima, 1992). Vogelmann (1989) pointed out that BSEs could modify the light microenvironment of the mesophyll layers because these transparent regions may create heterogeneous light gradients within leaves. Quartz fiber-optic microprobes were recently used to monitor the light gradients and the spectral regime along the BSE, as well as along the mesophyll of some representative heterobaric leaves (Karabourniotis et al., 2000). It was proposed that BSEs, apart from their water conducting (Wylie, 1943; Pizzolato et al., 1976; Mauseth, 1988; Fahn, 1990; Roth-Nebelsick et al., 2001), mechanical, and protecting (Wylie, 1943; Mauseth, 1988; Lucas et al., 1991; Turner, 1994a; Roth-Nebelsick et al., 2001) roles, behave as "transparent windows," transferring visible light to internal layers of mesophyll (Karabourniotis et al., 2000). It was also found that in certain plant species, the area corresponding to the transparent (and thus nonphotosynthetically

<sup>1</sup> This work was supported by the Greek Scholarship Foundation (postdoctoral scholarship to D.N.).

\* Corresponding author; e-mail karab@aua.gr; fax 1-5294286.

Article, publication date, and citation information can be found at [www.plantphysiol.org/cgi/doi/10.1104/pp.010943](http://www.plantphysiol.org/cgi/doi/10.1104/pp.010943).

active) regions being formed by the BSE might constitute a considerable portion of the total leaf area (Karabourniotis et al., 2000).

The present study addresses the following questions: Is there any correlation between leaf thickness and some critical anatomical parameters related to the occurrence of BSEs in heterobaric leaves? Is there any correlation between these parameters and photosynthetic capacity? Could the expression of photosynthetic capacity per unit of photosynthetically active leaf area or volume be used to interpret differences in the photosynthetic performance of heterobaric leaves? And does the anatomical character of BSEs confer an adaptive advantage related to the maintenance of adequate photosynthetic activity under stressful or unfavorable conditions?

## RESULTS

### Anatomical Characteristics of Heterobaric Leaves

Image analysis (see "Materials and Methods") was used to estimate the percentage of photosynthetically

active leaf area ( $A_p$ ) of the heterobaric leaves of a number of representative plant species, monocots or dicots. It was found that  $A_p$  is species dependent, ranging from 91% in *Malus sylvestris* to only 48% in *Gynerium* sp. (Table I). The non- $A_p$  of the leaves of all species examined corresponded to the transparent leaf area ( $A_t$ ; Fig. 1).  $A_t$  was positively correlated with leaf thickness ( $r^2 = 0.55$ ;  $P < 0.0001$ ; data not shown). Furthermore, the spatial characteristics of the transparent regions of the leaves could be represented in two ways: the transparent leaf area complexity factor ( $^{CF}A_t$ ; see "Materials and Methods" and Table II), which accounts for the length and the degree of branching (in dicots) or density (in monocots) of the BSEs, and the leaf transparent volume to total leaf surface ratio ( $\lambda_t$ ; see "Materials and Methods" and Table II), which represents the leaf volume occupied by transparent tissues per unit of leaf surface area.  $\lambda_t$  showed a strong correlation with leaf thickness (Fig. 2). The same trend was observed when the  $^{CF}A_t$  was plotted against leaf thickness ( $r^2 = 0.23$ ;  $P = 0.0006$ ; data not shown). In both cases, the regression was an

**Table I.**  $A_p$  (percentage of the total leaf area) and the photosynthetic capacity (expressed per unit of projected leaf area or per unit of  $A_p$ ) of the heterobaric leaves of 31 representative plant species

Values are means (six samples)  $\pm$  SE.

Species No.	Species	$A_p$ %	$P_{max}$ $\mu\text{mol O}_2 \text{ m}^{-2} \text{ s}^{-1}$	$P_{max}^*$ $\mu\text{mol O}_2 \text{ m}^{-2} A_p \text{ s}^{-1}$	Change %
1	<i>Acacia</i> sp.	81 $\pm$ 2.3	18.5 $\pm$ 0.9	22.8 $\pm$ 1.1	19.6
2	<i>Arbutus adrachne</i>	66 $\pm$ 2.8	52.0 $\pm$ 3.8	79.3 $\pm$ 5.8	34.2
3	<i>Arundo plinii</i>	66 $\pm$ 5.1	23.0 $\pm$ 1.8	35.1 $\pm$ 2.7	34.5
4	Oat ( <i>Avena sativa</i> )	77 $\pm$ 2.8	16.0 $\pm$ 1.4	20.7 $\pm$ 1.8	20.0
5	Judas Tree ( <i>Cercis siliquastrum</i> )	72 $\pm$ 2.7	16.6 $\pm$ 2.6	23.1 $\pm$ 3.6	27.8
6	Quince ( <i>Cydonia oblonga</i> )	89 $\pm$ 1.5	20.6 $\pm$ 1.8	23.1 $\pm$ 2.0	10.4
7	Japanese Plum ( <i>Eriobotrya japonica</i> )	83 $\pm$ 2.0	13.0 $\pm$ 0.9	15.7 $\pm$ 1.1	18.8
8	<i>Eucalyptus globulus</i>	74 $\pm$ 3.2	16.0 $\pm$ 1.9	21.6 $\pm$ 2.6	27.3
9	Fig ( <i>Ficus carica</i> )	83 $\pm$ 2.8	25.4 $\pm$ 1.1	30.6 $\pm$ 1.3	18.1
10	Cotton ( <i>Gossypium hirsutum</i> )	88 $\pm$ 2.6	41.0 $\pm$ 2.6	46.4 $\pm$ 2.9	12.8
11	<i>Gynerium</i> sp.	48 $\pm$ 2.9	25.0 $\pm$ 2.9	52.2 $\pm$ 6.1	51.9
12	Barley ( <i>Hordeum vulgare</i> )	81 $\pm$ 2.1	12.5 $\pm$ 0.9	15.4 $\pm$ 1.1	16.7
13	Walnut ( <i>Juglans regia</i> )	85 $\pm$ 2.4	15.6 $\pm$ 2.6	18.4 $\pm$ 3.1	13.3
14	Laurel ( <i>Laurus nobilis</i> )	76 $\pm$ 2.1	24.0 $\pm$ 2.1	31.6 $\pm$ 2.8	25.0
15	Apple ( <i>Malus sylvestris</i> )	80 $\pm$ 1.1	21.4 $\pm$ 3.9	26.8 $\pm$ 4.9	20.7
16	<i>Malva sylvestris</i>	91 $\pm$ 2.4	37.6 $\pm$ 3.2	41.5 $\pm$ 3.5	10.5
17	Mulberry ( <i>Morus alba</i> )	73 $\pm$ 2.1	16.0 $\pm$ 3.1	21.9 $\pm$ 4.2	27.3
18	<i>Nerium oleander</i>	76 $\pm$ 2.3	25.0 $\pm$ 2.4	32.9 $\pm$ 3.2	24.2
19	Pistachio Nut ( <i>Pistacia vera</i> )	82 $\pm$ 3.7	12.3 $\pm$ 1.1	15.0 $\pm$ 1.3	18.0
20	<i>Platanus orientalis</i>	81 $\pm$ 2.0	20.2 $\pm$ 1.1	24.8 $\pm$ 1.4	19.2
21	Almond ( <i>Prunus amygdalus</i> )	79 $\pm$ 2.1	27.4 $\pm$ 1.9	34.7 $\pm$ 2.4	21.7
22	Apricot ( <i>Prunus armeniaca</i> )	74 $\pm$ 5.7	24.0 $\pm$ 4.6	32.4 $\pm$ 6.2	27.3
23	Cherry ( <i>Prunus avium</i> )	83 $\pm$ 2.5	21.1 $\pm$ 1.1	25.4 $\pm$ 1.3	18.5
24	<i>Prunus damascena</i>	88 $\pm$ 0.8	24.0 $\pm$ 2.3	27.3 $\pm$ 2.6	11.1
25	Peach ( <i>Prunus persica</i> )	80 $\pm$ 2.1	27.5 $\pm$ 4.1	34.4 $\pm$ 5.1	21.4
26	Pear ( <i>Pyrus communis</i> )	76 $\pm$ 3.4	20.0 $\pm$ 5.0	26.3 $\pm$ 6.6	23.1
27	Kermes Oak ( <i>Quercus coccifera</i> )	58 $\pm$ 2.5	16.0 $\pm$ 2.1	27.6 $\pm$ 3.6	42.9
28	Holly Oak ( <i>Quercus ilex</i> )	78 $\pm$ 2.9	26.8 $\pm$ 3.2	34.4 $\pm$ 4.1	21.7
29	<i>Quercus alnifolia</i>	66 $\pm$ 2.8	34.9 $\pm$ 1.2	52.6 $\pm$ 1.8	33.6
30	Wheat ( <i>Triticum aestivum</i> )	81 $\pm$ 2.2	13.0 $\pm$ 1.1	16.0 $\pm$ 1.4	18.8
31	Grape ( <i>Vitis vinifera</i> )	76 $\pm$ 2.0	15.2 $\pm$ 1.5	20.0 $\pm$ 2.0	25.0

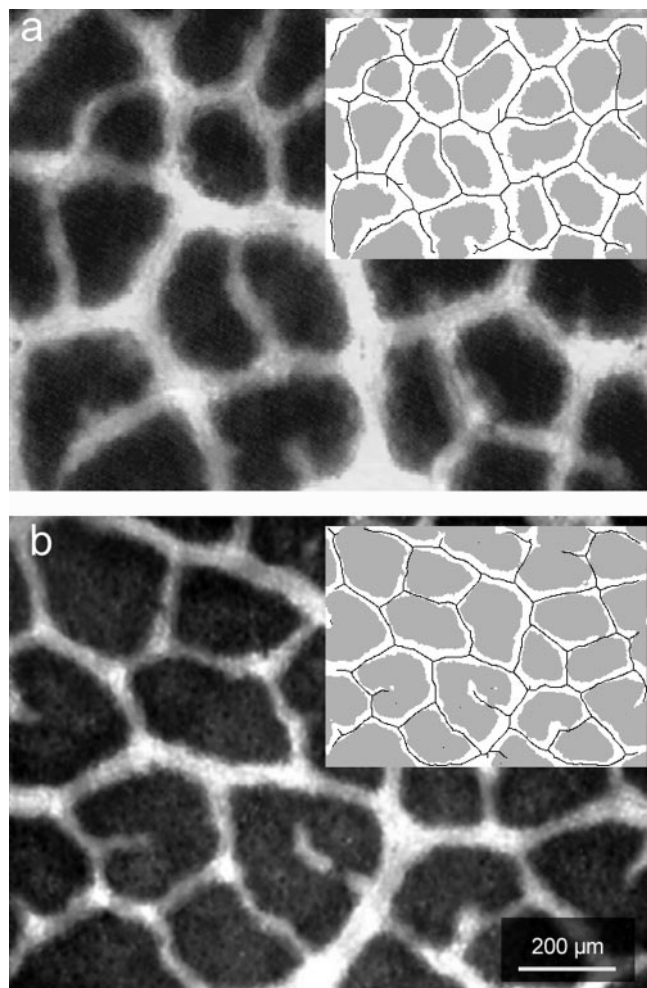


**Figure 1.** The abaxial surface of an intact leaf of *Q. coccifera* illuminated from the adaxial surface and viewed with a light microscope under low magnification. a, Sun-exposed leaf. b, Shade-exposed leaf. The inserts show the particular leaf area classes segmented by the image analysis procedure (see “Materials and Methods”). White region,  $A_t$ ; gray region,  $A_p$ ; solid line, trace of BSEs. The values of the particular parameters for these samples were: a, leaf thickness of 0.37 mm;  $A_p$  54.1%;  $\lambda_t$  0.084 mm<sup>3</sup> mm<sup>-2</sup>; and  $^{CF}A_t$  345 mm mm<sup>-2</sup>; b, leaf thickness of 0.25 mm;  $A_p$  73.6%;  $\lambda_t$  0.031 mm<sup>3</sup> mm<sup>-2</sup>;  $^{CF}A_t$  210 mm mm<sup>-2</sup>.

exponential curve. It was observed that the sharp break of the relationship between  $\lambda_t$  and leaf thickness was apparent at about 0.25 to 0.30 mm (Fig. 2). This was also the case for the correlations between  $A_t$  or  $^{CF}A_t$  and leaf thickness (data not shown).

Leaf thickness, apart from its species dependence, can be affected by several environmental factors. We tested the hypothesis that factors affecting the leaf thickness also affect anatomical traits of the heterobaric leaves related to the occurrence of the BSEs. Heterobaric leaves of three xeromorphic species developed under sun or shade conditions were chosen, and their anatomical traits were investigated. It was found that the expected modifications in leaf thickness under the two different light regimes were ac-

companied by large changes in  $A_p$ ,  $^{CF}A_t$ , and  $\lambda_t$  parameters (Table III; Fig. 1). The shade-developed leaves of the three species examined tended to be thinner, but their  $A_p$  was higher than that of the sun-developed ones. In accordance with this, the parameters related to the spatial characteristics of the BSEs ( $\lambda_t$  and  $^{CF}A_t$ ) of these leaves were higher in the sun-developed leaves compared with the shade-developed ones (Table III).

### Factors Affecting the Photosynthetic Performance of Heterobaric Leaves

As  $A_p$  ranged considerably between species, photosynthetic capacity expressed as oxygen evolution per unit projected leaf area ( $P_{max}$ ) should possibly follow a trend proportional to the percentage of the leaf area corresponding to the photosynthetically active parenchyma (i.e. the  $A_p$ ). Low  $A_p$  values were observed in leaves that possessed a high proportion of  $A_t$  and, consequently,  $P_{max}$  could be limited in those leaves. However, no correlation was revealed when  $P_{max}$  was plotted against  $A_t$  ( $r^2 = 0.00$ ;  $P = 0.7060$ ; data not shown). Such results could only be interpreted by the assumption that photosynthetic capacity expressed as oxygen evolution per unit of  $A_p$  ( $P_{max}^*$ ) is increased in leaves with low  $A_p$  values (thus leaves with high  $A_t$  values). According to Table I, species with similar  $P_{max}$  (e.g. *J. regia*,  $-15.6 \mu\text{mol m}^{-2} \text{s}^{-1}$  and *Q. coccifera*,  $-16 \mu\text{mol m}^{-2} \text{s}^{-1}$ ), but different  $A_p$  show significantly different  $P_{max}^*$  [18 and  $28 \mu\text{mol m}^{-2} \text{s}^{-1}$ , respectively]. In addition, a positive correlation was found between  $A_t$  of the examined species and  $P_{max}^*$  ( $r^2 = 0.18$ ;  $P = 0.0177$ ; data not shown). Moreover, using the spatial parameters described above to represent the  $A_t$  spatial characteristics (see previous section), a positive correlation was found between the  $^{CF}A_t$  (Fig. 3) or the  $\lambda_t$  and the  $P_{max}^*$  ( $r^2 = 0.23$ ;  $P = 0.0067$ ; data not shown). In addition,  $P_{max}$  was not correlated with leaf thickness ( $r^2 = 0.05$ ;  $P = 0.5024$ ; data not shown), whereas  $P_{max}^*$  has shown a much stronger correlation with the same parameter, following an exponential type curve ( $r^2 = 0.19$ ;  $P = 0.0570$ ; data not shown). The photosynthetic capacity per unit leaf volume ( $P_{max,v}^*$ ) of the heterobaric leaves of the 31 examined species followed the general trend (inverse first order) described by Roderick et al. (2000) in relation to the leaf thickness (data not shown). Moreover, the photosynthetic capacity per unit of photosynthetically active leaf volume ( $P_{max,v}^*$ ) showed an increased trend when leaf thickness exceeded 0.30 mm (data not shown). However, in both cases, the correlation was not statistically significant.

## DISCUSSION

### Factors Related to $A_p$ Spatial Characteristics

The data from image analysis showed that  $A_p$  as well as other related anatomical traits of the hetero-

**Table II.** List of symbols and definitions of terms used in the present study

Term	Symbol	Measurement Unit	Definition
Photosynthetically active leaf area	$A_p$	Percentage of the total leaf area	Leaf area that corresponds to photosynthetically active leaf tissue (obtained from image analysis)
Transparent leaf area	$A_t$	Percentage of the total leaf area	Leaf area that corresponds to nonphotosynthetically active leaf tissue (obtained from image analysis)
Transparent leaf area complexity factor	${}^{CF}A_t$	$\text{mm mm}^{-2}$	${}^{CF}A_t = {}^{T^1}\text{BSE} \times A_t$
Photosynthetic capacity per projected leaf area	$P_{\max}$	$\mu\text{mol O}_2 \text{ m}^{-2} \text{ s}^{-1}$	Obtained from leaf disk electrode measurements
Photosynthetic capacity per $A_p$	$P_{\max}^*$	$\mu\text{mol O}_2 \text{ m}^{-2} A_p \text{ s}^{-1}$	$P_{\max}^* = (P_{\max} \times 100/A_p)$
Photosynthetic capacity per unit leaf volume	$P_{\max,v}$	$\mu\text{mol O}_2 \text{ m}^{-3} \text{ s}^{-1}$	$P_{\max,v} = (P_{\max}/T)$
Photosynthetic capacity per unit of photosynthetically active leaf volume	$P_{\max,v}^*$	$\mu\text{mol O}_2 \text{ m}^{-3} V_p \text{ s}^{-1}$	$P_{\max,v}^* = (P_{\max,v} \times 100/V_p)$
Leaf thickness	$T$	mm	Obtained from image analysis
Bundle sheath extensions trace length	${}^{T^1}\text{BSE}$	$\text{mm mm}^{-2}$	Obtained from image analysis
Photosynthetically active leaf volume	$V_p$	Percentage of the total leaf volume	$V_p = A_p^a$
Transparent leaf volume	$V_t$	Percentage of the total leaf volume	$V_t = A_t^a$
Leaf transparent volume to total leaf surface ratio	$\lambda_t$	$\text{mm}^3 \text{ mm}^{-2}$	$\lambda_t = (V_t/A_s) = (A_t \times T/A_s)^b$

<sup>a</sup> Assuming that the BSEs are perpendicular to the leaf surface (see "Materials and Methods"). <sup>b</sup>  $A_s$  defined as the total leaf surface; see Roderick et al. (1999).

baric leaves are species dependent. Low  $A_p$  values were observed in xeromorphic species that are adapted to sunny and dry environments such as the Mediterranean one, where water availability may be the main limiting factor for plant growth. Under these conditions, small, thick (with low surface-to-volume ratio), and hard leaves are likely to be favored (Kummerow, 1973; Givnish, 1987; Turner, 1994a, 1994b). These attributes, although requiring a high construction cost in terms of carbon (Ehleringer and Mooney, 1983), permit the greatest carbon gain per unit transpirational loss (Givnish, 1987). Hardening is usually achieved by dense packing of the thick-walled mesophyll cells and the presence of thick protective and well-developed sclerenchymatous tissues. Thickening is usually achieved by adding more layers of palisade parenchyma cells (Kummerow, 1973; Turner, 1994a, 1994b). However, this type of leaf design could be unfavorable for the illumination of the internal layers of the spongy mesophyll cells if not accompanied by anatomical modifications (Vogelmann, 1993). According to Cui et al. (1991), in spinach (*Spinacia oleracea*) sun leaves, 90% of the collimated visible light at 450 nm was absorbed by the initial 120  $\mu\text{m}$  of photosynthetic parenchyma layers. In contrast, in the sclerophyllous sun leaves of *Q. coccifera*, 90% of the collimated visible light at 430 nm was absorbed by the initial 45  $\mu\text{m}$  of photosynthetic parenchyma layers (Karabourniotis et al., 2000). This means that the chlorophyll concentration profile of *Q. coccifera* leaves is denser than the corresponding one of spinach leaves. The anatomical construction of the BSEs, as well as their orientation, seems to favor light transferring to the neighboring mesophyll cells.

The occurrence of BSEs, acting as transparent "windows" that enrich the neighboring mesophyll areas with high levels of photosynthetically active radiation (PAR; Karabourniotis et al., 2000), probably enables considerable leaf thickening without the occurrence of a deficient light regime within internal mesophyll layers. Therefore, it is not surprising that species possessing heterobaric leaves tend to occur at sunny and dry sites, where water availability tends to be a limiting factor (Wylie, 1952; Terashima, 1992). In the present study, the anatomical parameters related to the occurrence of the BSEs were correlated with leaf thickness. Moreover, the exponential-type curves

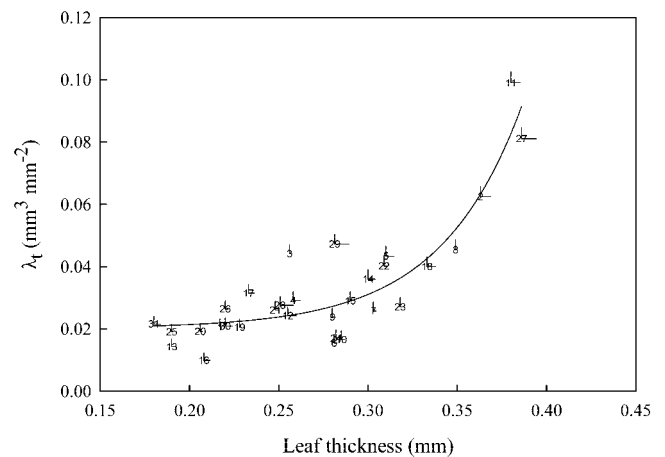


**Figure 2.** The regression [ $y = 0.02 + 1.55 \times 10^{-5} \times \exp(21.85 \times x)$ ;  $r^2 = 0.80$ ;  $P < 0.0001$ ] between the leaf thickness ( $x$ ) and the  $\lambda_t$  ( $y$ ) of the heterobaric leaves of 31 plant species. Species numbers are indicated in Table I. Points are means (six samples) and bars denote SE.

**Table III.** The leaf thickness,  $A_p$ ,  $\lambda_t$ , and  $^{CF}A_t$  of sun- and shade-exposed leaves of three representative Mediterranean evergreen sclerophyllous plants

Experimental details are in "Materials and Methods." Values are means (six samples)  $\pm$  SE.

Plant Species	Leaf Thickness			$A_p$			$\lambda_t$			$^{CF}A_t$		
	Sun	Shade	Change	Sun	Shade	Change	Sun	Shade	Change	Sun	Shade	Change
	mm		%	% of the total leaf area		%	$mm^3 mm^{-2}$		%	$mm mm^{-2}$		%
<i>Q. coccifera</i>	0.386 $\pm$ 0.008	0.242 $\pm$ 0.004	-37 <sup>a</sup>	58.0 $\pm$ 1.0	77.5 $\pm$ 1.7	25 <sup>a</sup> (46.4) <sup>b</sup>	0.081 $\pm$ 0.002	0.027 $\pm$ 0.002	-66 <sup>a</sup>	320 $\pm$ 11	174 $\pm$ 9	-46 <sup>a</sup>
<i>L. nobilis</i>	0.300 $\pm$ 0.004	0.227 $\pm$ 0.000	-24 <sup>a</sup>	76.1 $\pm$ 0.9	85.9 $\pm$ 0.3	11 <sup>a</sup> (41) <sup>b</sup>	0.036 $\pm$ 0.001	0.016 $\pm$ 0.000	-55 <sup>a</sup>	143 $\pm$ 5	68 $\pm$ 4	-52 <sup>a</sup>
<i>A. adrachne</i>	0.363 $\pm$ 0.006	0.299 $\pm$ 0.009	-18 <sup>a</sup>	65.2 $\pm$ 1.1	78.6 $\pm$ 1.4	17 <sup>a</sup> (38.5) <sup>b</sup>	0.063 $\pm$ 0.004	0.032 $\pm$ 0.002	-49 <sup>a</sup>	211 $\pm$ 12	102 $\pm$ 5	-52 <sup>a</sup>

<sup>a</sup> Highly significant differences ( $P < 0.01$ ). <sup>b</sup> The percentage of change of the corresponding transparent leaf area.

relating  $A_t$  (data not shown),  $\lambda_t$  (Fig. 2), or  $^{CF}A_t$  (data not shown) with leaf thickness indicate that the optical role of BSEs may only be essential in thick leaves. In actuality, a steep gradient is apparent in all the above relationships after 0.25 to 0.30 mm of leaf thickness. This is more or less the same leaf thickness at which there is an abrupt break in the general composition-morphology relationship for leaves (Roderick et al., 2000). There is presumably a need for structural and functional modifications in leaves thicker than 0.25 to 0.30 mm. Wylie (1939) has also found that vein density is related to the photosynthetic tissue organization, and that high vein density values are observed in leaves possessing high palisade-to-spongy mesophyll ratios (i.e. thick leaves). The 31 species could practically form two distinct groups based on the relation between leaf thickness and  $A_p$  spatial characteristics if the above limit is used; group I would bracket the species with leaf thickness up to 0.27 mm, and group II would bracket the species with leaf thickness higher than 0.27 mm. The majority of the 17 species of group II are xerophytic or mesophytic, possessing more or less sclerophyllous leaves, whereas the majority of the 14 species of group I are malacophyllous, mainly herbaceous species (Table I).

According to Wylie (1951), the mean spacing between BSEs is considerably higher in shade leaves than in thicker sun leaves. Similar results were obtained in the present study. The considerable thickening of the sun leaves of three Mediterranean evergreen sclerophylls was accompanied by a considerable reduction in their  $A_p$  as well as by increased values of the parameters related to the size (the  $\lambda_t$ ) and complexity (the  $^{CF}A_t$ ) of the leaf transparent tissues (Fig. 2; Table III). Therefore,  $A_p$  and the related parameters show not only interspecific variation as a consequence of species adaptation, but also intraspecific variation as a result of different illumination conditions or other potential environmental factors during leaf expansion. It also seems probable that in both cases, the determinate factor is leaf thickness or, according to Roderick et al. (2000), the leaf surface area-to-volume ratio. Similar modifications of the leaf functional anatomy have been observed in plants with leaves possessing sclereids that offer a light-guiding function. The number of sclereids per unit

leaf surface area in the evergreen sclerophyll species *Phillyrea latifolia* is significantly increased in the sun-exposed leaves when the leaf thickness tends to increase, compared with the shaded leaves (Karabourniotis, 1998). Therefore, it seems probable that maximum absorption may be more important for shade leaves than the moderation of the light gradient (Terashima and Hikosaka, 1995; DeLucia et al., 1996).

#### Relationship between $A_p$ Spatial Characteristics and Photosynthesis

Photosynthetic rates are commonly expressed as  $CO_2$  uptake or  $O_2$  evolution per unit of time per unit of projected leaf area. Using this basis of expression, variations in photosynthetic rates between plant species or varieties may be interpreted according not only to differences in stomatal or biochemical properties, but also according to the number and the arrangement of the photosynthetically active cells per unit leaf surface area (Nobel, 1991; Austin, 1992). In heterobaric leaves, photosynthetic parenchyma cells cover a much smaller portion of the leaf surface compared with homobaric leaves and thus, a loss in photosynthetic potential of these leaves (as  $P_{max}$ ),

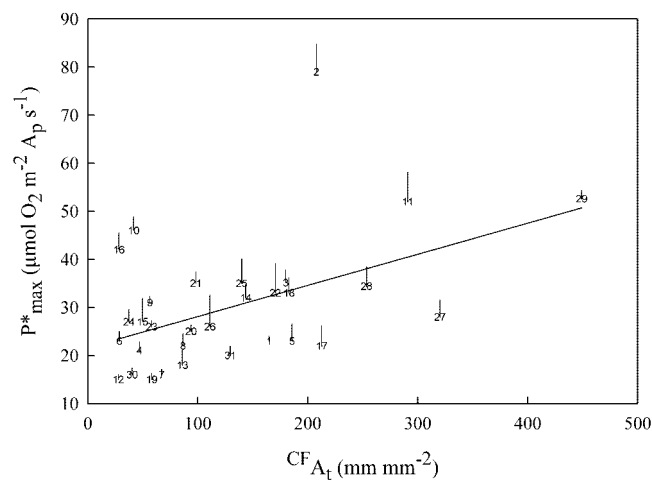


**Figure 3.** The linear regression ( $r^2 = 0.23$ ;  $P = 0.0063$ ) between the  $^{CF}A_t$  and the  $P_{max}^*$  of the heterobaric leaves of 31 plant species. Other details as in Figure 2.

proportional to their  $A_t$  values, is expected. However, according to the results of the present study,  $P_{\max}$  of these leaves was not considerably affected by the size of their  $A_t$ . Thus, the decrease in  $A_p$  is expected to be compensated by an increase in  $P_{\max}^*$ , probably through the light enrichment of each areole. In the present study, species possessing significantly different  $A_p$  (like *Q. coccifera* and *J. regia*) showed similar  $P_{\max}^*$ . It is obvious that the photosynthetic tissue of *Q. coccifera* functions more efficiently in terms of  $P_{\max}^*$  than that of *J. regia*, probably due to the additional photosynthetic parenchyma layers, but also due to more efficient enhancement of the light microenvironment within mesophyll of these thick and compact leaves (Karabourniotis et al., 2000). Therefore, it seems important that the area corresponding to the network of the transparent regions of each heterobaric leaf determines to some extent their photosynthetic capacity. However, the area corresponding to the BSE probably is not the only factor that plays an important role. The improvement of the light microenvironment of the photosynthetic parenchyma layers due to the light transferring function of the BSE may depend not only on the area, but also on the density and/or the portion of leaf volume occupied by these structures.  $P_{\max}^*$  showed a positive correlation with  $\lambda_t$  and  $^{CF}A_t$ . Thus, the expression of  $P_{\max}^*$  allowed the interpretation of the photosynthetic performance of the heterobaric leaves in relation to some critical anatomical traits. In conclusion, the area, the volume, and the density of BSEs affect, to some extent, the photosynthetic capacity, and that is apparent only if the latter is expressed on a  $A_p$  basis.

Leaves of evergreen trees and shrubs are considered to have very low photosynthetic capacities relative to those of crop and herbaceous plants (Evans, 1989; Lambers and Poorter, 1992; Hikosaka et al., 1998). However, according to McClendon (1992), the occurrence of prominent BSEs is more frequent in trees than in herbaceous plants. It has been also proposed that Mediterranean-climate sclerophylls exhibit low photosynthetic capacities compared with many mesomorphic species (Ehleringer and Mooney, 1983; Turner, 1994a; Larcher, 1995). Yet the increased venation and probably the occurrence of BSEs, as an anatomical trait, characterize the leaves of these plants (Archibold, 1995). According to the results of the present study, the referred variations in photosynthetic capacities between some plant groups may be interpreted, at least in part, by the particular anatomical traits of species possessing heterobaric leaves. Thus, the interpretation of correlations of photosynthesis expressed on a projected leaf area or volume basis to structural (e.g. specific leaf area [SLA], leaf thickness, etc.) or other biochemical and physiological leaf traits, should take into account the different underlying mechanisms or structural com-

plexities of the particular leaves (e.g. homobaric or heterobaric).

According to McClendon (1962),  $P_{\max}$  is positively correlated with the leaf density thickness (i.e. leaf fresh mass per unit projected area), but that study did not provide any further information about the kind of the leaves examined (heterobaric or homobaric). In our study,  $P_{\max}^*$  was correlated with leaf thickness, but  $P_{\max}$  did not show a similar trend. In addition, the increasing trend followed by  $P_{\max,v}^*$  when leaf thickness exceeded 0.30 mm suggests that the optical role of the BSEs is only essential in thick leaves. Thus, the occurrence of high photosynthetic rates in thick leaves could be facilitated by an increase of the  $A_t$  or transparent leaf volume.

Stomatal patchiness may be an unavoidable by-product of the rather advantageous heterobaric leaf anatomy (Canny, 1990; Nonami et al., 1990; Beyschlag and Eckstein, 1998). It has been suggested that the cause of the patchy stomatal closure might be the heterogeneous water status in different parts of the leaf (Terashima, 1992; Beyschlag and Eckstein, 1998). Although the existence of the BSEs creates a more uniform light environment within each areole, the light regime between different areoles may vary due to the different leaf inclination within the canopy. On the other hand, the relative independence of each areole could permit a different status regarding photosynthetic activity in response to the light intensity as well as stomatal conductance and, therefore, could alter the water status in each compartment. As a result, the developing differences in water status due to the non-uniform photosynthesis could act as a feedback control point in each compartment.

The findings of the present study corroborate the views that the heterobaric leaf anatomy may offer advantages. The existence of BSEs appears to be an adaptation in saving water and in protecting mesophyll against water stress (Terashima, 1992). The unavoidable reduction of the photosynthetic capacity per projected leaf area of heterobaric leaves due to the occurrence of transparent regions may be compensated from higher photosynthetic rates per  $A_p$ , due to a higher light availability within mesophyll and/or the occurrence of additional layers of photosynthetic parenchyma cells. The net profit seems to be an improved water economy and a more effective light distribution per areole.

The results of the present study clearly show that variations in certain anatomical-morphological factors of heterobaric leaves contribute to the interpretation of interspecific differences in photosynthetic capacity. However, SLA and nitrogen content are also important factors determining the photosynthetic capacity of the leaves. Numerous ecophysiological studies have showed that independent from differences in climate, soil conditions, and evolutionary history among diverse life forms, there are interspecific relationships between these factors and the

photosynthetic performance (Lambers and Poorter, 1992; Reich et al., 1997; Poorter and Evans, 1998; Niimets, 1999; Roderick et al., 1999). Thus, one may predict the particular photosynthetic capacity from the SLA and nitrogen concentration of the leaves. Therefore, it would be of interest to examine these relationships among the two different functional groups of leaves (homobaric and heterobaric) and to compare the different structural strategies in respect to the photosynthetic performance.

## MATERIALS AND METHODS

### Plant Material and Sampling Sites

All experiments were performed during the summer of 1998. All cultivated plants were collected from the Agricultural University experimental plantation. The sun and shade leaves of *Quercus coccifera*, *Laurus nobilis*, and *Arbutus adrachne* were collected from naturally grown individuals on Mount Parnis, near Athens, in a mixed pine-oak forest at a 500-m elevation. Sun leaves were collected from plants growing in an open habitat receiving an irradiance of 2,000  $\mu\text{mol photons m}^{-2} \text{s}^{-1}$  PAR at midday. Shade leaves (100–200  $\mu\text{mol photons m}^{-2} \text{s}^{-1}$  PAR) were collected from plants growing in the pine forest understory or in the interior of the plant canopy. The distance between all sampling sites was less than 300 m. Light intensity measurements were taken by a quantum sensor (LI-188B; LI-COR, Lincoln, NE). In all cases, the leaves were wrapped in plastic bags, put into a portable coolbox, and taken immediately to the laboratory for further measurements.

### Microscopic Observations and Image Analysis

An Axiolab Zeiss light microscope (Carl Zeiss, Jena, Germany) equipped with a color CCD camera (ICD-840P RGB; Ikegami Tsushinki, Tokyo) was used for all microscopical observations. Measurements of leaf thickness were taken from hand-cut cross sections of fresh leaves. In pubescent leaves such as those of *Quercus ilex* and *Quercus alnifolia*, the thickness of the trichome layer was included in the measurement because it is considered to be optically functional (Karabourniotis and Bornman, 1999; and see Karabourniotis et al., 1999).

Digital images of the leaf lamina were taken from fresh leaf disc preparations fixed between two microscopic slides, using transmitted light, and were captured with a video board (Pinnacle PCTV; Pinnacle Systems, Braunschweig, Germany) in a PC system as 24-bit red-green-blue with a resolution of 640 by 480 pixels. Images were converted to 8-bit gray-scale files and stored in tagged image file format.

Measurements of leaf area classes (i.e.  $A_p$  and  $A_t$ ) were made with image analysis software (Image-Pro Plus, version 3.01, Media Cybernetics, Silver Spring, MD) by the following procedure: each image was converted to binary by selecting an appropriate gray-scale value threshold level. The output image was compared with the initial color image to ensure that the discrimination of the leaf

surface classes was satisfactory.  $A_p$  and  $A_t$  were calculated as the percentage of the total leaf area (Fig. 1, inserts). The estimation of the two leaf surface classes was based on the assumption that the projected leaf image upon transmitting light is a representation of the mean distribution of the two types of leaf tissues, i.e. the photosynthetic tissue and the transparent tissue. In all cases, the estimation of  $A_t$  and  $A_p$  for each species was accompanied by validation using the corresponding cross sections. As a consequence, we assumed that the limits between the two types of tissues are defined by imaginary planes, which are linear and perpendicular to the lamina level.

The  $^{CF}A_t$  was calculated by multiplying  $A_t$  by BSEs trace length ( $^{TL}BSE$ ). Measurements of the  $^{TL}BSE$  were made with a custom computer program developed in Matlab (version 5.1.0.421, Mathworks Inc., Natick, MA) according to the following steps: A manual threshold level was selected so as to convert the gray-scale images to binary. All BSE traces were displayed while the noise from the  $A_p$  was kept to a minimum; the limits between the two area classes were smoothed by a noise-reduction filter; small, isolated white objects resulting from random noise were eliminated by an effacement filter; all BSE traces were reduced to a minimum width (1 pixel) by a morph filter; and due to conversion of the BSE areas to one-dimension lines in the previous step, side tails were produced on the traces. For this reason, a second morph filter was used to eliminate all 20-pixel length portions. The final images were composed by single-dimensional (i.e. one pixel wide) objects, which represented the traces of the BSEs (Fig. 1, inserts).  $^{TL}BSE$  was calculated from the output value after calibration with samples of known length and were expressed as  $\text{mm mm}^{-2}$  leaf area. The computer program is available from the authors on request.

$\lambda_t$  was calculated as the transparent leaf volume-to-leaf surface area ratio. The transparent leaf volume was calculated by multiplying  $A_t$  by leaf thickness. Leaf surface area was calculated according to Roderick et al. (1999).

For the expression of  $P_{\text{max},v}^*$ , photosynthetically active leaf volume was calculated by multiplying  $A_p$  by leaf thickness. Terms, symbols, and definitions used in the present study are listed in Table II.

### Other Measurements

Photosynthetic capacity was measured with a leaf disc oxygen electrode (Hansatech Instruments, King's Lynn, UK) at 30°C under 1,500  $\mu\text{mol m}^{-2} \text{s}^{-1}$  PAR. Because non-uniform photosynthesis over the area of the heterobaric leaves may be attributed to patchy stomatal closure (Terashima, 1992), photosynthetic rates were measured at saturating (5%, w/v)  $\text{CO}_2$  concentration to overcome stomatal limitations (Terashima, 1992; Walker, 1993).

### Statistics

A two-tailed *t* test was used to determine statistically significant differences in the measurement parameters be-

tween samples. Correlation coefficients were determined by regression analysis.

#### ACKNOWLEDGMENTS

We thank Prof. G. Theodoropoulos and the Computer Center of the National Technical University of Athens for the use of computer programs. We also thank Dr. Ourania Georgiou and Dr. Theofanis Konstadinidis for naming the plant species.

Received October 15, 2001; returned for revision November 16, 2001; accepted January 22, 2002.

#### LITERATURE CITED

- Archibold OW** (1995) Ecology of World Vegetation. Chapman and Hall, London
- Austin RB** (1992) Plant productivity and genetic variation in photosynthesis. *In* J Barber, MG Guerrero, H Medrano, eds, Trends in Photosynthesis Research. Intercept Lim, Andover, UK, pp 319–338
- Beyschlag W, Eckstein J** (1998) Stomatal patchiness. *Prog Bot* **59**: 283–298
- Canny MJ** (1990) What becomes of the transpiration stream? *New Phytol* **114**: 341–368
- Cui M, Vogelmann TC, Smith WK** (1991) Chlorophyll and light gradients in sun and shade leaves of *Spinacia oleracea*. *Plant Cell Environ* **14**: 493–500
- DeLucia EH, Nelson K, Vogelmann TC, Smith WK** (1996) Contribution of intercellular reflectance to photosynthesis in shade leaves. *Plant Cell Environ* **19**: 159–170
- Ehleringer J, Mooney HA** (1983) Productivity of desert and Mediterranean-climate plants. *In* OL Lange, PS Nobel, CB Osmond, H Ziegler, eds, Encyclopedia of Plant Physiology, New Series, Vol 12D. Springer-Verlag, Berlin, pp 205–231
- Esau K** (1977) Anatomy of Seed Plants. John Wiley & Sons, New York
- Evans GR** (1989) Photosynthesis and nitrogen relationships in leaves of C3 plants. *Oecologia* **78**: 9–19
- Fahn A** (1990) Plant Anatomy. Pergamon Press, Oxford
- Givnish TJ** (1987) Comparative studies of leaf form: assessing the relative roles of selective pressures and phylogenetic constraints. *New Phytol* **106**: 131–160
- Hikosaka K, Hanba YT, Hirose T, Terashima I** (1998) Photosynthetic nitrogen-use efficiency in leaves of woody and herbaceous species. *Funct Ecol* **12**: 896–905
- Karabourniotis G** (1998) Light-guiding function of foliar sclereids in the evergreen sclerophyll *Phillyrea latifolia*: a quantitative approach. *J Exp Bot* **49**: 739–746
- Karabourniotis G, Bornman JF** (1999) Penetration of UV-A, UV-B and blue light through the leaf trichome layers of two xeromorphic plants, olive and oak, measured by optical fiber microprobes. *Physiol Plant* **105**: 655–661
- Karabourniotis G, Bornman JF, Liakoura V** (1999) Different leaf surface characteristics of three grape cultivars affect leaf optical properties as measured with fiber optics: possible implication in stress tolerance. *Aust J Plant Physiol* **26**: 47–53
- Karabourniotis G, Bornman JF, Nikolopoulos D** (2000) A possible optical role of the bundle sheath extensions of some heterobaric leaves. *Plant Cell Environ* **23**: 423–430
- Karabourniotis G, Papastergiou N, Kabanopoulou E, Fasseas C** (1994) Foliar sclereids of *Olea europaea* may function as optical fibers. *Can J Bot* **72**: 330–336
- Krulik GA** (1980) Light transmission in window-leaved plants. *Can J Bot* **58**: 1591–1600
- Larcher W** (1995) Physiological Plant Ecology. Springer-Verlag, Berlin
- Kummerow J** (1973) Comparative anatomy of sclerophylls of Mediterranean climatic areas. *In* F di Castri, HA Mooney, eds, Mediterranean Type Ecosystems: Origin and Structure, Ecological Studies 7. Springer-Verlag, Berlin, pp 157–167
- Lambers H, Poorter H** (1992) Inherent variation in growth rate between higher plants: a search for physiological causes and ecological consequences. *Adv Ecol Res* **23**: 187–261
- Lucas PW, Choong MF, Tan HTW, Turner IM, Berrick AJ** (1991) The fracture toughness of the leaf of the dicotyledon *Calophyllum inophyllum* L. (Guttiferae). *Philos Trans R Soc London B* **334**: 95–106
- Mandoli DF, Briggs WR** (1982) Optical properties of etiolated plant tissues. *Proc Natl Acad Sci USA* **79**: 2902–2906
- Mandoli DF, Briggs WR** (1984a) Fiber optics in plants. *Sci Am* **251**: 90–98
- Mandoli DF, Briggs WR** (1984b) Fiber-optic plant tissues: spectral dependence in dark-grown and green tissues. *Photochem Photobiol* **39**: 419–424
- Mauseth JD** (1988) Plant Anatomy. The Benjamin/Cummings Publication Company, Menlo Park, CA
- McClendon JH** (1962) The relationship between the thickness of deciduous leaves and their maximum photosynthetic rate. *Am J Bot* **49**: 320–322
- McClendon JH** (1992) Photographic survey of the occurrence of bundle-sheath extensions in deciduous dicots. *Plant Physiol* **99**: 1677–1679
- Niinemets Ü** (1999) Components of leaf dry mass per area—thickness and density—alter leaf photosynthetic capacity in reverse directions in woody plants. *New Phytol* **144**: 35–47
- Nobel PS** (1991) Physiological and Environmental Plant Physiology. Academic Press, San Diego
- Nonami H, Schulze ED, Ziegler H** (1990) Mechanisms of stomatal movement in response to air humidity, irradiance and xylem water potential. *Planta* **183**: 57–64
- Pizzolato TD, Burbano JL, Berlin JD, Morey PR, Pease RW** (1976) An electron microscope study of the path of water movement in transpiring leaves of cotton (*Gossypium hirsutum* L.). *J Exp Bot* **27**: 145–161
- Poorter H, Evans JR** (1998) Photosynthetic nitrogen—use efficiency of species that differ inherently in specific leaf area. *Oecologia* **116**: 26–37
- Reich PB, Walters MB, Ellsworth DS** (1997) From tropics to tundra: global convergence in plant functioning. *Proc Natl Acad Sci USA* **94**: 13730–13734



- Roderick ML, Berry SL, Noble IR** (2000) A framework for understanding the relationship between environment and vegetation based on the surface area to volume ratio of leaves. *Funct Ecol* **14**: 423–437
- Roderick ML, Berry SL, Noble IR, Farquar GD** (1999) A theoretical approach to linking the composition and morphology with the function of leaves. *Funct Ecol* **13**: 683–695
- Roth-Nebelsick A, Uhl D, Mosbrugger V, Kerp H** (2001) Evolution and function of leaf venation architecture: a review. *Ann Bot* **87**: 553–566
- Terashima I** (1992) Anatomy of non-uniform leaf photosynthesis. *Photosynth Res* **31**: 195–212
- Terashima I, Hikosaka K** (1995) Comparative ecophysiology of leaf and canopy photosynthesis. *Plant Cell Environ* **18**: 1111–1128
- Turner IM** (1994a) Sclerophylly: primarily protective? *Funct Ecol* **8**: 669–675
- Turner IM** (1994b) A quantitative analysis of leaf form in woody plants from the world's major broadleaved forest types. *J Biogeogr* **21**: 413–419
- Vogelmann TC** (1989) Penetration of light into plants. *Photochem Photobiol* **50**: 895–902
- Vogelmann TC** (1993) Plant tissue optics. *Annu Rev Plant Physiol Plant Mol Biol* **44**: 231–251
- Walker DA** (1993) Polarographic measurement of oxygen. *In* DO Hall, JMO Scurlock, HR Bolhar-Nordenkamp, RC Leegood, SP Long, eds, *Photosynthesis and Production in a Changing Environment: A Field and Laboratory Manual*. Chapman & Hall, London, pp 91–112
- Wylie RB** (1939) Relations between tissue organization and vein distribution in dicotyledon leaves. *Am J Bot* **26**: 219–225
- Wylie RB** (1943) The role of the epidermis in foliar organization and its relations to the minor venation. *Am J Bot* **30**: 273–280
- Wylie RB** (1951) Principles of foliar organization shown by sun-shade leaves from ten species of deciduous dicotyledonous trees. *Am J Bot* **38**: 355–361
- Wylie RB** (1952) The bundle sheath extension in leaves of dicotyledons. *Am J Bot* **39**: 645–651